

Photoacoustic Tomography of a Nanoshell Contrast Agent in the in Vivo Rat Brain

Yiwen Wang,[†] Xueyi Xie,[†] Xueding Wang,[†] Geng Ku,[†] Kelly L. Gill,[‡]
D. Patrick O'Neal,[‡] George Stoica,[§] and Lihong V. Wang^{*,†}

Optical Imaging Laboratory, Department of Biomedical Engineering, Texas A&M University, College Station, Texas 77843-3120, Nanospectra Biosciences, Inc., Houston, Texas 77054, and Department of Pathobiology, Texas A&M University, College Station, Texas 77843-5547

Received June 8, 2004

ABSTRACT

This study demonstrates the feasibility of using nanoshells in vivo as a new contrast-enhancing agent for photoacoustic tomography. Deep penetrating near-infrared light was employed to image the in vivo distribution of poly(ethylene glycol)-coated nanoshells circulating in the vasculature of a rat brain. The images, captured after three sequential administrations of nanoshells, present a gradual enhancement of the optical absorption in the brain vessels by up to 63%. Subsequent clearance of the nanoshells from the blood was imaged for ~6 h after the administrations.

Introduction. Optical imaging techniques aided by contrast agents have high sensitivity and specificity. During the past decade, imaging of perfusion of optical contrast agents, such as cyanine dyes¹ and nanoparticles,² has become a standard tool for studying the functions of and diagnosing disorders in living tissues. Photoacoustic tomography (PAT), a novel hybrid imaging modality that combines the merits of both light and ultrasound, has proven to be a powerful technique for visualizing tissue structures and functions with high contrast, good spatial resolution, and satisfactory imaging depth.^{3–5} PAT is suitable for monitoring exogenous optical contrast agents as well.⁶

A nanoshell is a new kind of optically tunable nanoparticle, consisting of a dielectric core (silica) surrounded by a thin metallic layer (gold). By adjusting the size of the nanoparticle core relative to the thickness of the gold shell, the optical resonance of nanoshells can be precisely and systematically varied over a broad spectrum including the near-infrared (NIR) region where the optical transmission through biological tissues is optimal. In contrast to NIR absorbing dyes, the absorption properties of nanoshells are dependent upon a rigid metallic structure rather than on molecular orbital electronic transitions. Nanoshells are also not susceptible to

photobleaching, a problem commonly associated with other such structures.

The nanoshells surface, gold, is a chemically inert material well-known for its biocompatibility.^{7–11} In addition, polymers such as poly(ethylene glycol) (PEG) can be grafted to nanoshell surfaces in self-assembled monolayers. It has been demonstrated that PEG-coated liposomes suppress immunogenic responses thus improving blood circulation times.^{12,13}

Recently, nanoshells have been applied in a simple thermal therapy for subcutaneous murine tumors.¹⁴ Nanoshells as well as other long-circulating small (60–400 nm dia.) particles tend to extravasate and accumulate in tumors via a passive mechanism referred to as the “enhanced permeability and retention effect,”¹⁵ which is attributed to dysfunctional anatomical conditions such as localized leaky circulatory and lymphatic systems. In contrast, healthy vessels in the brain (e.g., the blood-brain barrier) are well-known for their ability to dissuade the extravasation of such particles. Contrast agents currently in clinical use, such as those used in conjunction with magnetic resonance imaging, take advantage of this difference. The end result of this type of nanoshell accumulation is greatly enhanced NIR optical contrast in the vicinity of a tumor vasculature. Our thermal therapy employs a NIR laser to preferentially heat the nanoshells and destroy the tumor by several thermal mechanisms, including, but not limited to, anti-angiogenesis effects, induced immune response, and gross hyperthermia. The integration of an

* Corresponding author. E-mail: lwang@tamu.edu; tel: 979-847-9040; fax: 979-845-4450.

[†] Department of Biomedical Engineering, Texas A&M University.

[‡] Nanospectra Biosciences, Inc.

[§] Department of Pathobiology, Texas A&M University.

imaging tool such as PAT to characterize and monitor the accumulation of nanoshells in situ would be an invaluable aid in the further refinement of this therapeutic technique.

In this study, we explored the feasibility of metal nanoshells as an intravascular contrast agent for PAT of living animals. The vasculature in a rat brain, with enhanced optical contrast created by nanoshells, was imaged in vivo with a high spatial resolution by PAT for the first time to our knowledge. This technology allowed us to monitor the dynamics of the nanoshells in the circulatory system of the rat.

Methods. Silica nanoparticles of 125 ± 5 nm in diameter were obtained (MP-1040, Nissan Chemical America Corporation) and suspended in ethanol. The particle surface was then terminated with amine groups by reaction with 3-aminopropyltriethoxysilane (APTES, 97+%, Avocado Research Chemicals, Ltd.). Small gold colloid (1–3 nm dia.) was grown using the method of Duff et al.¹⁶ This colloid was aged for 4–7 days at 6 °C and then concentrated using a rotary evaporator. The aminated silica particles were then added to the gold colloid suspension. Gold colloid is adsorbed to the amine groups on the silica surface, resulting in a silica nanoparticle covered with islands of gold colloid. Gold–silica nanoshells were then grown by reacting HAuCl_4 (Sigma-Aldrich) with the silica–colloid particles in the presence of formaldehyde. This process reduces additional gold onto the colloid that is already adsorbed on the silica particle surface. These colloidal islands serve as nucleation sites, causing the surface colloid to grow, eventually coalescing with neighboring colloids, to form a complete metal shell. The nanoshell optical properties were assessed using a UV–vis spectrophotometer (Genesys 5, Spectronic, Inc.). The resulting nanoshell solutions had a 10–12 nm thick gold shell, which generated a peak optical absorption at 800 ± 5 nm (see Figure 1A), a wavelength that exhibits optimal penetration into scattering biological tissues. Nanoshell surfaces were coated with PEG by combining aqueous 25 μM PEG-SH (5000 MW PEG-SH, Nektar) with nanoshells (8.0×10^9 nanoshells/mL) in deionized water in an argon atmosphere, which was followed by centrifugation to remove residual PEG-SH from the nanoshell formulation. Prior to injection, the PEGylated nanoshells were sterilized using a 0.22 μm syringe filter and resuspended at 2.0×10^{11} nanoshells/mL concentration in sterile 0.9% saline solution. This “stealthed” nanoshell formulation was measured to have a half-life of ~ 3.7 h in the blood of immune-competent BALB/C mice in separate experiments at Nanospectra Biosciences, Inc.

The setup for noninvasive PAT of the rat brain with an optical contrast agent is shown in Figure 1. An Nd:YAG laser (Brilliant B, Bigsky), operating at a wavelength of 532 nm with a fwhm of 6.5 ns and a pulse repetition rate of 10 Hz, was utilized to pump a tunable dye laser (ND6000, Continuum) to generate short laser pulses at a wavelength of 800 nm. We immobilized the rat on a custom animal mount which exposed its head into a water tank through an opening at the bottom of the tank, the opening of which was sealed using a sheet of clear polyethylene film. When the

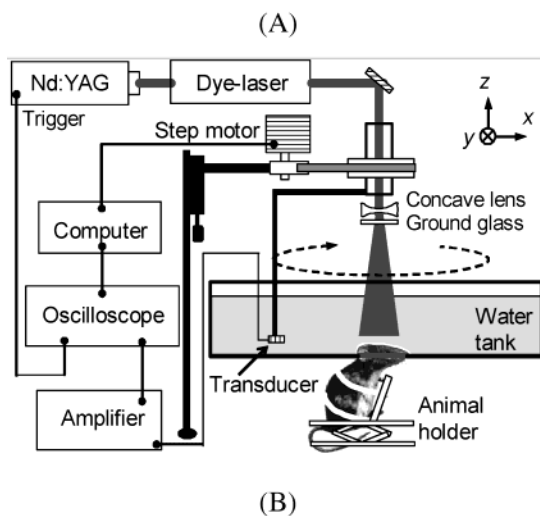
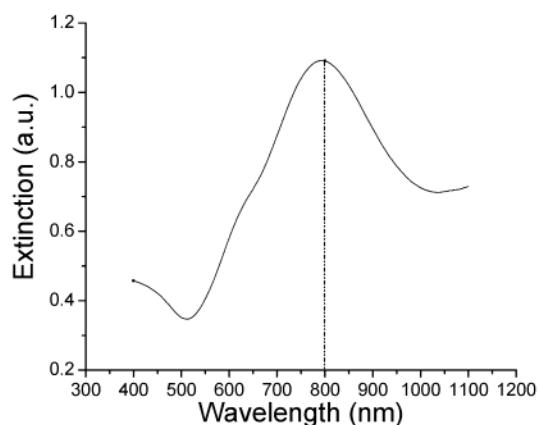


Figure 1. (A) Extinction spectrum of the nanoshell solution, where the peak absorbance is at 800 nm. (B) Schematic of the noninvasive PAT of the rat brain in vivo, employing the nanoshell contrast agent and NIR light.

laser beam irradiates the rat’s head, a small temperature rise (< 5 mK) in the tissue causes thermoelastic expansion that produces photoacoustic waves. A nonfocused ultrasonic transducer (XMS-310, Panametrics) with a central frequency of 10.4 MHz, a bandwidth of 100% at ~ 6 dB, and an active element of 2 mm in diameter was submerged in the water to detect the photoacoustic signals. A revolving detection system was driven by a computer-controlled stepper motor to rotate the transducer around the cortical surface of the rat brain with a radius of 3 cm and a step size of 1.5 deg. The data acquisition time to obtain a single 2-D image slice was ~ 24 min. The photoacoustic signals detected by the transducer were amplified by a low-noise preamplifier before being fed to a digital oscilloscope (TDS 540B, Tektronix), which digitized the photoacoustic signals. Finally, a computer acquired the signals and stored the data for image reconstruction. A modified back-projection algorithm was employed to reconstruct the brain images from the photoacoustic signals.^{17,18} The spatial resolution of this imaging system, limited mainly by the bandwidth of the detected photoacoustic signals, is $\sim 60 \mu\text{m}$.¹⁹

Sprague Dawley rats (130–160 g body weight, Charles River, Wilmington, MA) were employed in this work.

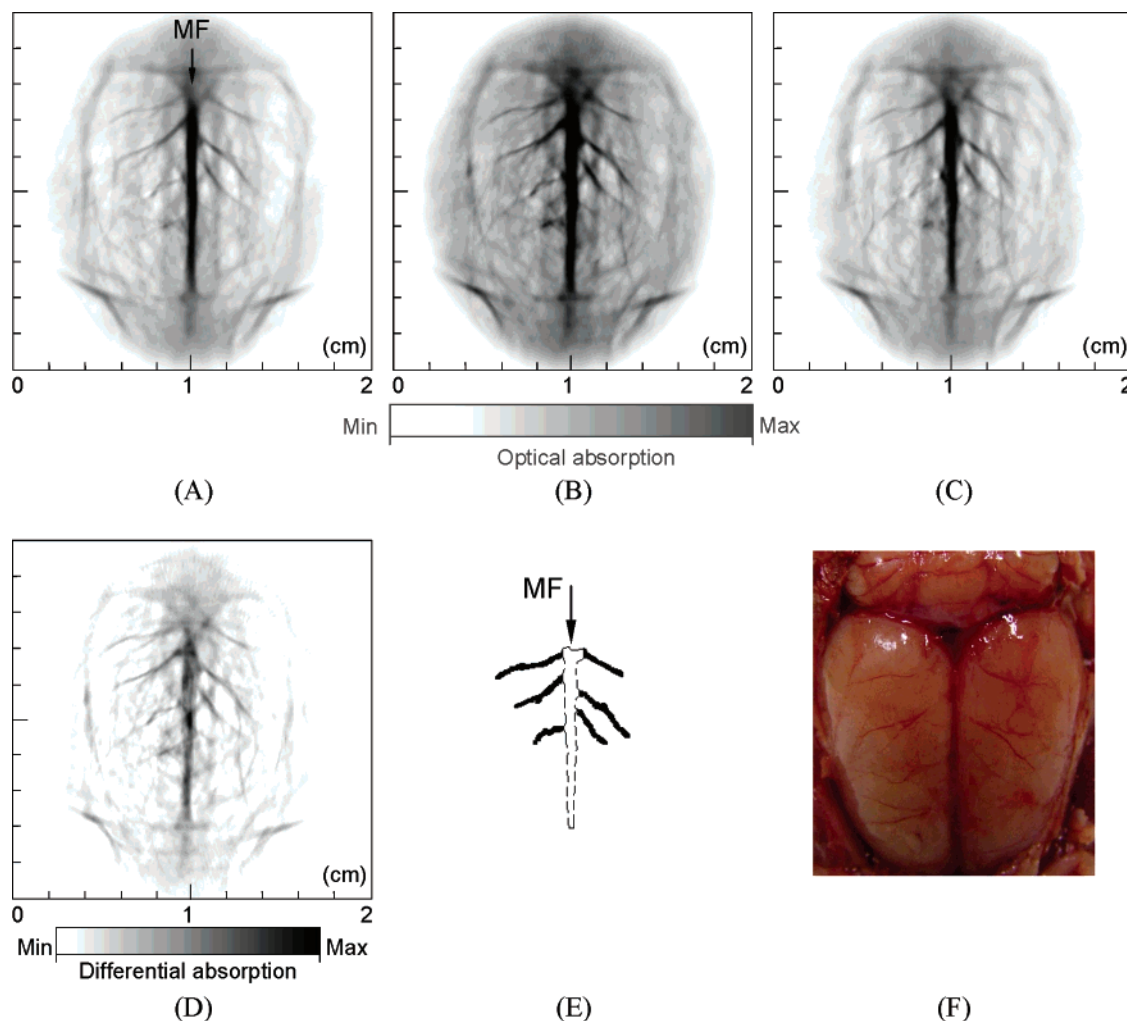


Figure 2. Noninvasive PAT of a rat brain in vivo employing the nanoshell contrast agent and NIR light at a wavelength of 800 nm. (A) Photoacoustic image acquired before the administrations of nanoshells. *MF*: median fissure. (B) Photoacoustic image obtained ~ 20 min after the third administration of nanoshells. (C) Photoacoustic image acquired ~ 350 min after the third administration of nanoshells. (D) Differential image that was obtained by subtracting the pre-injection image from the post-injection image (Image D = Image B – Image A). (E) Large blood vessels in the cerebral cortex segmented from the PAT images (shown with solid regions). (F) Open-skull photograph of the rat brain cortex obtained after the data acquisition for PAT.

General anesthesia was administered on the rat by an intramuscular injection of ketamine hydrochloride (44 mg/kg), xylazine hydrochloride (2.5 mg/kg), acepromazine maleate (0.75 mg/kg), and atropine (0.025 mg/kg). As required, the initial anesthesia was maintained with additional half-doses of the intramuscular agents during placement of a tail vein catheter (26 gauge, 19 mm long; Abbocath-T; Abbott Ireland, Sligo, Ireland). During the procedure, the rat was placed on a water-circulating heating pad (Gaymar T/pump; Gaymar Industries, Orchard Park, NY), and additional heating was provided by an overhead surgical lamp. Before imaging, the hair on the rat head was removed gently with an over-the-counter depilatory lotion. During the data acquisition, the rat was provided pure oxygen for breathing and the arterial blood oxygenation (SpO₂) level and heart rate were monitored by a pulse oximeter (8600 V, NONIN) with the fiberoptic probe wrapped around a paw of the animal. The SpO₂ level was $\sim 90\%$ and the heart rate was ~ 350 bpm throughout the experiment, which showed that the rat was in good condition throughout the procedure.

The tail vein of the rat was catheterized and three successive injections of nanoshells were administered, each at a dose of $\sim 0.8 \times 10^9$ nanoshells/g body weight. Image acquisition of the rat brain cortex began approximately 5 min following each administration. After the last nanoshell injection, the rat brain was imaged 10 times sequentially over a period of ~ 6 h. After the data acquisition for imaging, the rat was euthanized by pentobarbital overdose (120 mg/kg, IP) and its open-skull anatomy was photographed.

Results and Discussion. Three of the photoacoustic angiographs of the cerebral cortex of the rat brain are presented in Figures 2A, B, and C, where the color bars are identical. Compared to the brain image based on the intrinsic optical contrast (Figure 2A), the image acquired ~ 20 min after the third administration of the nanoshell contrast agent (Figure 2B) shows the brain vasculature with greater clarity. With the exogenous contrast agent, the optical absorption of the blood was increased and the contrast between the vessels and the background brain tissues was enhanced. The brain image in Figure 2C was acquired ~ 6 h after the third

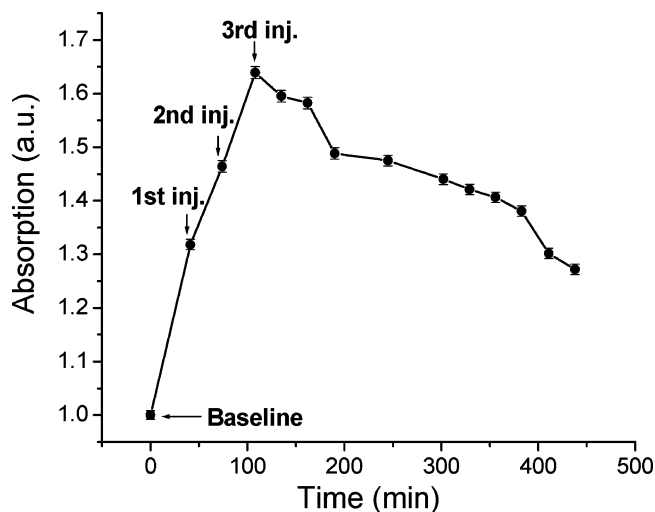


Figure 3. The averaged optical absorption in the segmented vessels, normalized to the averaged intrinsic optical absorption before the first administration, as a function of time. The vertical error bars indicate the range of estimations.

administration of nanoshells. Due to the clearance of the nanoshells from the blood, the optical absorption in the blood vessels decreased significantly. The differential image in Figure 2D is a result of the subtraction of the pre-injection image in Figure 2A from the post-injection image in Figure 2B. This image depicts the distribution of differential optical absorption in the rat brain induced by the exogenous contrast agent. All of the PAT images of the rat brain match well with the open-skull anatomical photograph in Figure 2F.

In all of the PAT images, six large blood vessels were segmented (Figure 2E). The optical absorptions in the segmented areas are averaged to quantify the concentration of the nanoshells in the circulatory system of the rat (Figure 3). During the three administrations, the optical absorption in the blood vessels increased gradually due to the increased concentration of nanoshells in the blood. The first administration increased the absorption of the blood by $\sim 30\%$. The three administrations combined increased the absorption of the blood by 63% . From the 11 images acquired continuously after the third administration, we can see a gradual decrease in the optical absorption in the brain vessels as a result of the clearance of the nanoshells from the blood.

After the first administration of the nanoshells, the concentration of nanoshells in the blood is estimated to be $\sim 1 \times 10^{10}$ nanoshells/mL. Considering that the spatial resolution of this PAT system in the imaged cross-section is $\sim 60 \mu\text{m}$ and the diameters of the cortical blood vessels under study are less than $100 \mu\text{m}$, the number of nanoshells in the $60 \times 60 \times 100 \mu\text{m}^3$ resolvable volume is ~ 3600 , which approximates the sensitivity of this PAT system.

The optical absorption of whole blood at the 800-nm wavelength is $\sim 5 \text{ cm}^{-1}$. On the condition that the scattering of nanoshells in the blood is minimal, the administered

nanoshell dose of 1×10^{10} nanoshells/mL concentration in the blood is expected to increase the optical absorption in the blood vessels by $\sim 100\%$. As a result, the estimated enhancement of optical absorption is greater than that observed by the PAT system.

Summary. Employing laser-based PAT, we successfully imaged the dynamic distributions of gold nanoshells, a novel nanoparticle contrast agent with a tunable absorption spectrum, in the rat brain in vivo with high spatial resolution and satisfactory sensitivity. PAT of exogenous nanoparticles can potentially provide an accurate noninvasive method to monitor the intravascular or extravascular fluid pathways in biological samples. For example, imaging the perfusion of nanoparticle contrast agents in vascular systems will potentially permit the accurate assessment of acute ischaemic stroke, lesion development, thermal injury, neovascularization, tumor angiogenesis, tumor necrosis, hepatic function, and regional hemodynamic activities. By employing nanoparticles conjugated to bioactive materials such as proteins, antibodies, and drugs, this technique will potentially enable molecular imaging and therapeutic monitoring. Finally, we expect that the further development of an imaging tool such as PAT to characterize and monitor the accumulation of nanoshells in vivo will be applied to the detection of tumors in situ as well as to guiding nanoshell-based thermal tumor therapy.

References

- (1) Li, X.; Beauvoit, B.; White, R.; Nioka, S.; Chance, B.; Yodh, A. *SPIE Proc.* **1995**, 2389, 789–797.
- (2) Rouillat, M. H.; Russier-Antoine, I.; Benichou, E.; Brevet, P. F. *Anal. Sci.* **2001**, 17, 235.
- (3) Wang, X.; Pang, Y.; Ku, G.; Xie, X.; Stoica, G.; Wang, L. V. *Nat. Biotechnol.* **2003**, 21(7), 803–806.
- (4) Wang, X.; Pang, Y.; Ku, G.; Stoica, G.; Wang, L. V. *Opt. Lett.* **2003**, 28(19), 1739–1741.
- (5) Kruger, R. A.; Reinecke, D. R.; Kruger, G. A. *Med. Phys.* **1999**, 26, 1832–1837.
- (6) Wang, X.; Ku, G.; Wegiel, M. A.; Bornhop, D. J.; Stoica, G.; Wang, L. V. *Opt. Lett.* **2004**, 29, 730–732.
- (7) West, J. L.; Halas, N. J. *Annu. Rev. Biomed. Eng.* **2003**, 5, 285–92.
- (8) Hirsch, L. R.; Jackson, J. B.; Lee, A.; Halas, N. J.; West, J. L. *Anal. Chem.* **2003**, 75, 2377–81.
- (9) Jackson, J. B.; Westcott, S. L.; Hirsch, L. R.; West, J. L.; Halas, N. J. *Appl. Phys. Lett.* **2003**, 82, 257.
- (10) Prodan, E.; Halas, N. J.; Nordlander, P. *Chem. Phys. Lett.* **2003**, 368, 94–101.
- (11) Schwartzberg, A. M.; Grant, C. D.; Wolcott, A.; Zhang, J. Z. *SPIE Proc.* **2003**, 5221, 100–107.
- (12) Chen, A. M.; Scott, M. D. *BioDrugs* **2001**, 15, 833–847.
- (13) Harris, J. M.; Martin, N. E.; Modi, M. *Clin. Pharmacokinet.* **2001**, 40, 539–551.
- (14) O’Neal, D. P.; Hirsch, L. R.; Halas, N. J.; Payne, J. D.; West, J. L. *Cancer Lett.* **2004**, 209, 171–176.
- (15) Maeda, H.; Fang, J.; Inutsuka, T.; Kitamoto, Y. *Int. Immunopharmacol.* **2003**, 3, 319–328.
- (16) Duff, D. G.; Baiker, A. *Langmuir* **2003**, 9, 1993–2301.
- (17) Xu, M.; Xu, Y.; Wang, L. V. *IEEE Trans. Biomedical Eng.* **2003**, 50(9), 1086–1099.
- (18) Xu, M.; Wang, L. V. *Phys. Rev. E* **2003**, 67(5), 056605, 1–15.
- (19) Ku, G.; Wang, L. H. *Med. Phys.* **2000**, 27, 1195–1202.

NL049126A